Hindawi
International Journal of Corrosion
Volume 2019, Article ID 5470646, 7 pages
https://doi.org/10.1155/2019/5470646

Research Article

Epoxy Resin's Influence in Metakaolin-Based Geopolymer's Antiseawater Corrosion Performance

Wenrui Bian,[1] Zhongchang Wang ,[1,2] and Mo Zhang[1]

[1]*Tunnel and Underground Structure Engineering Center of Liaoning, Dalian Jiaotong University, Dalian, Liaoning Province, 116028, China*
[2]*School of Traffic and Transportation Engineering, Dalian Jiaotong University, Dalian, Liaoning Province, 116028, China*

Correspondence should be addressed to Zhongchang Wang; wazoch@163.com

Received 24 February 2019; Revised 27 May 2019; Accepted 12 June 2019; Published 3 July 2019

Guest Editor: Yuxin Wang

To obtain the influence mechanism of epoxy resin content, curing time, and other external factors on the compressive strength and seawater corrosion resistance of geopolymer, the NaOH and Na_2SiO_3 were used as activators; the effect of epoxy resin concentration on the corrosion resistance of metakaolin-based geopolymer was investigated by experiments. The mechanism of epoxy resin concentration affecting the polymerization process and the properties of geopolymer was analyzed by X-ray diffraction, scanning electron microscopy-energy spectrum, and Fourier transform infrared spectroscopy. It was shown that the epoxy resin slowed down the polymerization. The presence of epoxy resin had a beneficial effect on compact structure. Furthermore, compared with the noncorrosive specimen, mixed with 30% specimen's average compressive strength increased by 4.77MPa and 4.24MPa after curing for 1d and 3d and soaking for 56d.

1. Introduction

With the economic development of the Yangtze River Delta, the Pearl River Delta and the Bohai Bay region, more and more coastal infrastructures were built. However, the concrete structures are prone to be corroded in marine environment. The repair costs are high [1]. Improving corrosion resistance of offshore concrete structures is becoming more and more important. Current methods to prevent corrosion are mainly considered in the design stage, material selection, concrete mix design, adequate compaction, curing and anticorrosion coatings [2]. The traditional anticorrosive coatings such as epoxy anticorrosive coatings, rubber anticorrosive coatings, and polyurethane anticorrosive coatings had large solvent pollution, short antiseptic life, and poor weather resistance. The modified coatings did not change the internal structure and could not have excellent properties [3–7].

Geopolymers were an inorganic polymer formed by $\{SiO_4\}^{4-}$ and $\{AlO_4\}^{5-}$ first used by J. Davidovits in the late 1970s [8]. As emerging cementations materials, geopolymers have their great mechanical properties with low CO_2 emission and low energy consumption. The reaction of synthetic geopolymers requires metakaolin or raw silicoaluminates. The CO_2 emission can be reduced by 20% [9, 10]. Some industrial waste with amorphous silicon aluminum structure can be used to synthesize geopolymers, for example, metakaolin, fly ash, red mud, and granulated blast furnace slag [11]. The metakaolin has become the best aluminosilicate material owing to its high rate of dissolution in the reactant solution [12–14]. Geopolymer based materials have excellent mechanical properties, high early strength, freeze-thaw resistance, low chloride diffusion rate, abrasion resistance, and thermal stability [9, 15, 16]. Geopolymer has lower calcium content and stronger acid corrosion resistance than traditional cement [17]. Geopolymers as anticorrosive coatings are seldom studied. Ana María Aguirre-Guerrero et al. used impressed voltage and wetting/drying (w/d) cycles in the presence of a 3.5% NaCl solution to investigate the MK based geopolymer had better corrosion resistance [18]. Zhang et al. obtained good corrosion resistance by using a liquid-solid ratio of 90% metakaolin and 10% blast furnace slag at a liquid-solid ratio of 0.6 ml/g. It was necessary to add polypropylene (PP) fiber and MgO expansion agent to improve dry shrinkage properties of geopolymers. The

Table 1: Chemical composition of MK.

Material	SiO_2	Al_2O_3	Fe_2O_3	TiO_2	K_2O	Na_2O	CaO	MgO	LOI
Content(wt.%)	49.67	42.54	1.32	2.14	0.18	0.68	0.19	0.40	2.74

Table 2: The phase corresponding to XRD Atlas.

Symbol	Mineral name	Chemical formula
a	Nepheline	$NaAlSiO_4$
b	Sodium aluminosilicate	$Na_2O\ Al_2O_3\ SiO_2$
c	Sodium feldspar	$NaAlSi_3O_8$
d	Hydrate sodium aluminosilicate	$NaSiAlO_4\ H_2O$
e	quartz	SiO_2
f	Cubicite	$Na(Si_2Al)O_6\ H_2O$

geopolymer could be a new type of green anticorrosion coating. Its development in anticorrosion coating is limited due to its drawbacks of large shrinkage and easy cracking [19].

In order to solve the issues previously described and to improve the geopolymers' technologic properties, in the paper geopolymers containing epoxy resins with different mass ratio had been produced. Moreover, in order to investigate the morphology and the interface interactions between the geopolymers and the epoxy resins, a detailed microstructural analysis was performed.

2. Materials and Methods

2.1. Materials. The metakaolin (MK) from Jiaozuo Yu Kun Mining Co., Ltd. in Henan province was used as the raw material for geopolymer synthesis. The composition of MK was listed in Table 1. The Na_2SiO_3 (SiO_2/Na_2O molar ratio 2.0) was from a chemical plant in Hebei province, and the NaOH was from Dalian. The epoxy resin was from a chemical plant in Zhejiang province. The seawater was taken from the offshore waters of Dalian Heishijiao Park.

2.2. Specimen Preparation. The mixture of 50% NaOH and Na_2SiO_3 solution with SiO_2/Na_2O molar ratio 2.0 was used as the activator. The mass ratio of epoxy resin was 0%, 10%, 20%, and 30%, respectively.

The activator and metakaolin were mixed and stirred for 10min. Then, epoxy resin was added and continued to mix for 5 minutes. The slurry was poured into cylindrical molds and vibrated for 30 seconds for preparing φ37mm×750mm cylinder samples. Then, the slurry was sealed in zip bags and curing under room temperature until unconfined compression tests. Based on the ratios of epoxy resin (0%, 10%, 20%, and 30%), EGP0, EGP10, EGP20, and EGP30 were used.

2.3. Mechanical and Microstructural Characterization

2.3.1. Anticorrosion Performance Test. The anticorrosion performance was mainly determined by the compressive strength under different curing time and corrosion time under different resin dosages. To investigate the compression strength of the Epoxy Geopolymer (EGP), the unconfined compression test was conducted on a universal testing machine. The constant loading rate was 0.0788 in./min. To reduce the effect of uneven surface formed during curing, the top surface of sample was covered with a cardboard.

2.3.2. Microstructural Characterization. To observe the microscopic morphological changes of epoxy resin geopolymer samples after seawater corrosion, SEM scanning of selected samples was performed by JSM-6360LV scanning electron microscope. The 5×5×5mm cubic specimen was trimmed off from the center of the destroyed specimen. After drying, the sample was placed on the alumina stud with conductive adhesive for coating with gold-palladium alloy.

2.3.3. Mineralogy Characterization. The mineralogical changes of the epoxy resin geopolymer samples after seawater corrosion were analyzed using an Empyrean X-ray diffractometer. The main purpose of the XRD test was to determine whether the geopolymer precursor and the epoxy resin had undergone a chemical reaction and whether the geopolymer had reacted with seawater. This can be done by observing whether a new peak (new mineral) was produced on the map. CuKα radiation was used and analyzed by MDI Jade 5.0 (see Table 2) .

3. Results and Discussion

3.1. Mechanical Properties of Different Resin-Doped Geopolymers. The compressive strength data of the resin blends at 0%, 10%, 20%, and 30% for 1d, 3d, and 28d was shown in Figure 1. The compressive strength of EGP0-EGP30 after curing for 1d was 15.32MPa, 11.376MPa, 10.04MPa, and 7.90MPa, respectively. The strength of EGP0 was 7.42MPa higher than the strength of EGP30, and the compressive strength of EGP0 was 4.17MPa higher than the strength of EGP30 after curing for 28d. The compressive strength growth rate of EGP0-EGP30 group after curing for 28 days compared with curing for 3d was 18.52%, 49.12%, 57.04%, and 65.34%, respectively.

The effect of resin on the compressive strength of geopolymer was as follows. With the increase of resin content, the compressive strength of geopolymer decreased gradually.

Table 3: Infrared vibration peaks of metakaolin and geopolymer.

Wavenumber	Assignment
3700-3600	Stretching vibration (OH)
3600-2200	Stretching vibration(OH,HOH)
1700-1600	Bending vibration(HOH)
1430-1410	Stretching vibration(O C O)
1200-950	Non-symmetric stretching vibration (T O Si, T= Si, Al)
1100	Non-symmetric stretching vibration(Si O Si)
800-780	Symmetric stretching vibration(Si O Si)
424-470	Bending vibration(Si O Si and O Si O)

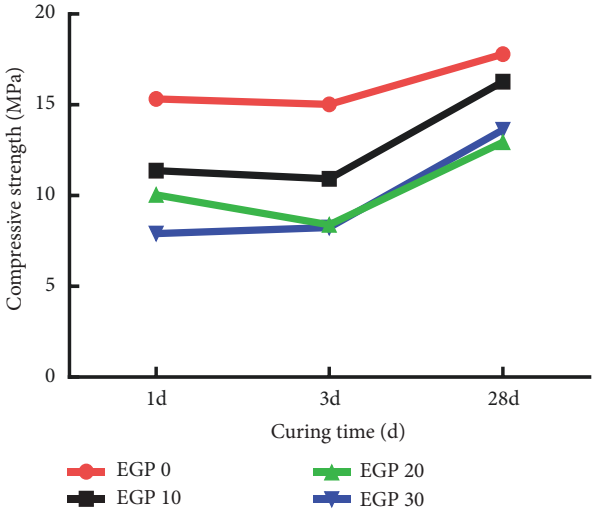

Figure 1: Compressive strength of different resin content in curing for 1d, 3d, and 28d.

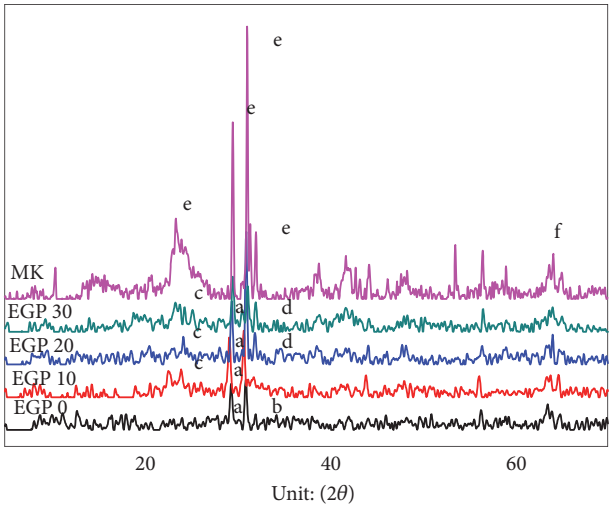

Figure 2: XRD patterns of different resin content geopolymers and metakaolin.

This may be because there were a large number of small bubbles in the resin, but the bubbles were not completely discharged after mixing and vibration exhaust. With the increase of resin content, the number of bubbles increased, and the internal structure of geopolymer was more loose. The effect of curing time on the compressive strength of geopolymer was as follows. With the increase of the curing time, the compressive strength of geopolymer increased gradually, but with the increase of resin content after 3 days of curing, the increase rate of the compressive strength of geopolymer increased gradually.

The geopolymer without epoxy resin will achieve high compressive strength after 1d of curing, which was due to the rapid reaction of the metakaolin base precursor. In the early stage of curing, the polycondensation reaction was completed, so that the strength was increased, and the epoxy resin will be doped into the alkali excitation solution to hinder the reaction. So the compressive strength of geopolymer which mixed epoxy resin would be improved in the later curing times.

3.2. Mineralogy Characterization. The X-ray diffraction (XRD) spectrum of the epoxy resin metakaolin geopolymer curing 28 d was shown in Figure 2. It can be seen that the composition of metakaolin was mainly an amorphous structure. Compared with the metakaolin, the geopolymers' peaks at 2θ 25° and 30° were gradually weakened, and the phase corresponding to the e peak was quartz phase, indicating that the quartz phase was decreasing. However, two peaks c and d appeared in EGP10-EGP30, which may be caused by incomplete reaction; the aluminosilicate dissolved in an alkaline solution and formed a hydroxylated chain product without proceeding. The water molecules were decomposed between the chain products to form a three-dimensional network structure. This also explains why the strength of the geopolymer increased as the soaking time increases. There was no significant change in the pattern after the addition of epoxy resin (no new minerals were formed), so the compressive strength was largely determined by the geopolymer gel.

3.3. Score FTIR Spectra of Epoxy Resin, Metakaolin, and Geopolymer with Different Epoxy Resin Concentrations. According to the existing research, the functional groups represented by the infrared vibration peak are shown in Table 3 [20, 21].

Compared to the metakaolin, it can be seen from Figures 3 and 4 that the geopolymer has 4 more obvious

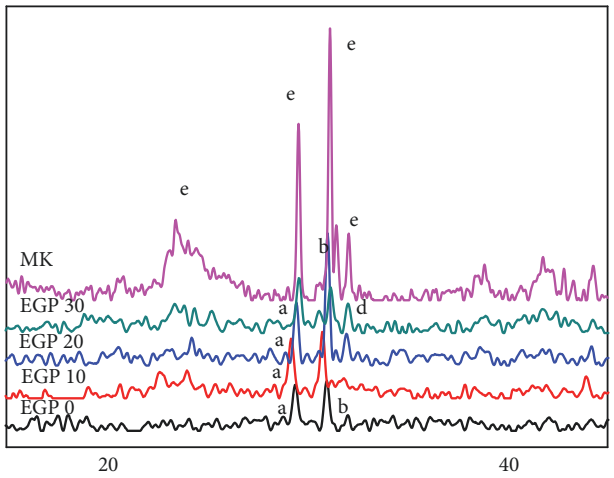

Figure 3: 20°-40° XRD patterns of different resin content geopolymers and metakaolin.

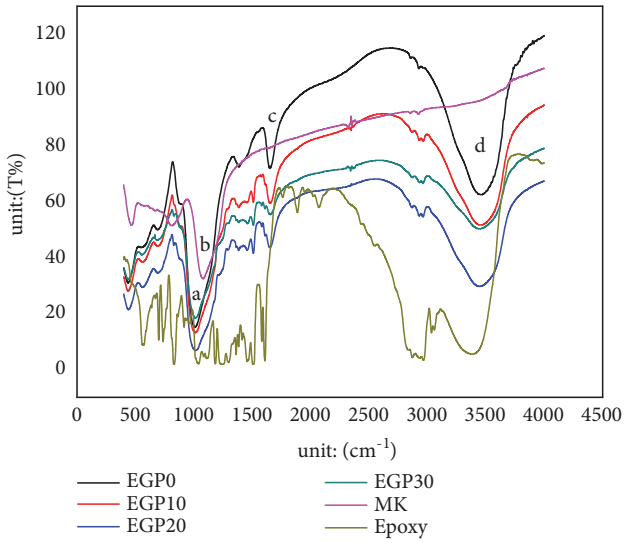

Figure 4: Score FTIR spectra of epoxy resin, metakaolin, and geopolymer with different epoxy resin concentrations.

peaks: a (1000 cm^{-1}), b (1050 cm^{-1}), c (1590 cm^{-1}), and d (3400 cm^{-1}). As shown in Figure 5 with the metakaolin, there was no e (811 cm^{-1}) peak, and e represented Al-O, so it indicated that metakaolin had been dissolved in the solution. The peaks a and b represented the vibration of the asymmetric functional group T-O-Si (T was Si or Al) since the energy contained in the Si atom was larger than the energy contained in the Al atom. The vibration moves in the direction of the low wave number as the Al atom composition in the structure increases. Compared with the metakaolin, geopolymers' T-O-Si (T:Sior Al) shifted to the a peak, and it indicated all groups formed geopolymer gel. However it could be seen from Figure 5 that the EGP20 vibrated most obviously at a, so it had more Si-O-Al, because of the Si-O-Si chemical bond had higher strength, so the EGP20's had the lowest compressive strength. The c peak belongs to the bending

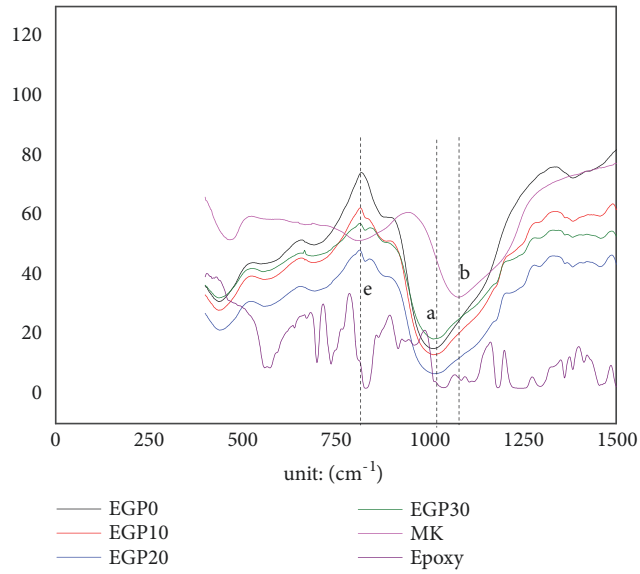

Figure 5: Partial enlarged detail of a and b.

Table 4: Silicon-aluminum ratio of geopolymers with different resin content.

	EGP 0	EGP 10	EGP 20	EGP 30
Si/Al	1.91	2.11	2.36	2.58

vibration of HOH. The vibration peak showed the bound water and interlayer water entrained inside the geopolymer after the reaction, and it could be seen that the peak vibration was weakened as the amount of the resin was increased. This could be inferred that the resin slowed down the evaporation of water molecules after the geopolymerization. The -OH stretching vibration of the peak d reflected a hydroxyl group-containing gel in which the inside of the geopolymer did not undergo a polycondensation reaction after dissolution [22, 23].

3.4. SEM Image and Energy Spectrum Analysis of Geopolymers. The microscopic morphology of the fracture surface of different resin-doped geopolymers after curing 28d was shown in Figure 6. It can be seen from Figure 6 that the white matter was a nonconducting material, the spherical one was epoxy resin, and the other irregular ones were metakaolin or other impurities. The EGP0 geopolymer's microstructure was dense, and the gel formed a homogeneous whole. After adding epoxy resin, geopolymer's microstructure was loose; therefore, the compressive strength decreased after adding the resin. But the epoxy resin was embedded in the gel and formed a whole.

Table 4 shows the ratio of silicon to aluminum of the polymer in different resin dosages. When the ratio of silicon to aluminum was in the range of 2-3, it was very close to the pure geopolymer gel, which indicated that the epoxy resin only inhibited the progress of the reaction.

The ratio of silica to aluminum with different resin content was shown in Table 4. The gel can be divided into

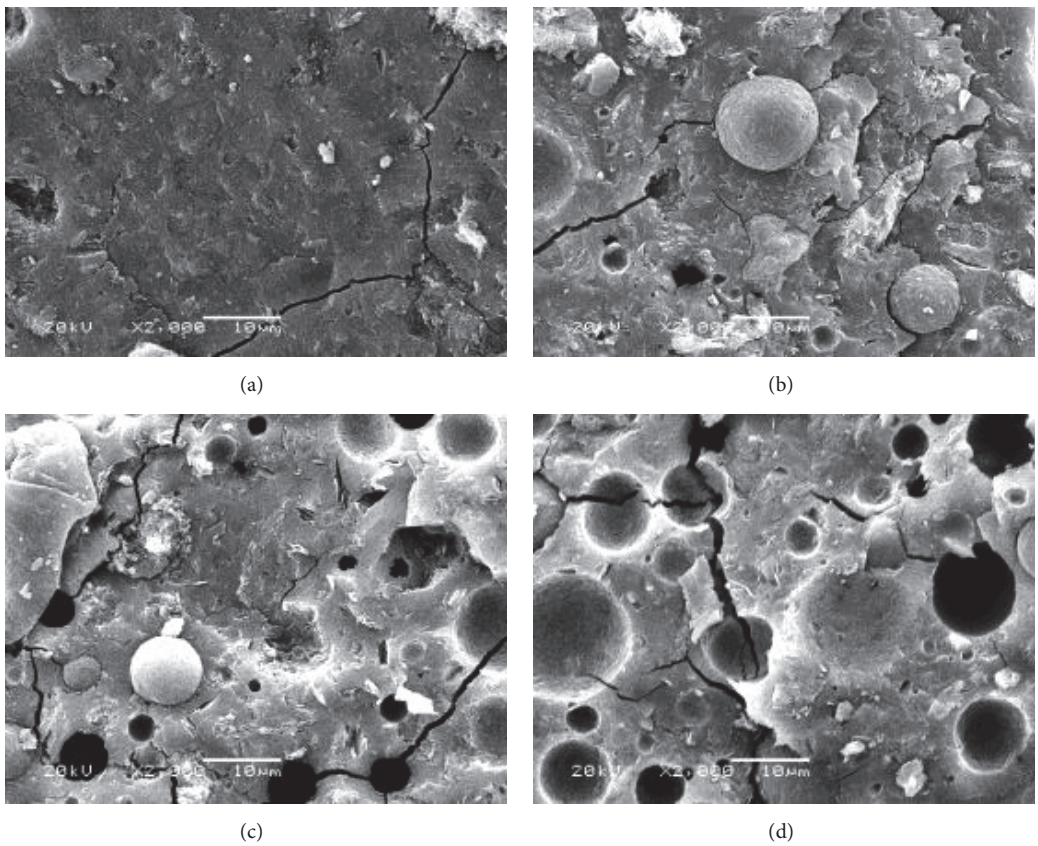

Figure 6: (a), (b), (c), and (d) represented the SEM images of EGP 0, EGP 10, EGP 20, and EGP 30 after curing for 28 days.

the PS, PSS, and PSDS gel according to the ratio of Si to Al. From the ratio of Si to Al, it was known that the PSS was the main type of gel when no epoxy resin was added, and with the increase of epoxy resin, the PSDS type was the main type of gel. It can be explained that the formation of polymer gel without hindering the addition of epoxy resin merely slowed down the reaction time.

3.5. Corrosion Resistance of Geopolymers. It can be seen from Figure 7 that the compressive strength of EGP 0 decreased, which is not related to the length of curing time. This is because alkali-exciting solution is basically completed when EGP 0 was curing 1d. The compressive strength also reached a higher level. The compressive strength of EGP10 and EGP20 did not change much with the soaking time after curing for 1d and 3d. The compressive strength of EGP10 and EGP20 decreased with the soaking time after curing for 28d. However, the strength of EGP 30 decreased by 4.94 MPa with the immersion time after curing for 28d, but the compressive strength increased with the immersion time during the curing time of 1d and 3d (the compressive strength was enhanced by 4.77 MPa and 4.24 MPa, respectively). This may be due to the fact that the structure becomes denser after the addition of the epoxy resin, the corrosion resistance can be excellent, or the seawater inhibited the polycondensation reaction, resulting in a slow increase in strength.

3.6. Mineralogy Characterization. The effect of seawater immersion on the compressive strength of geopolymers was as follows. After curing for 1d and 3d, as the soaking time increased, the compressive strength of the geopolymer gradually decreased. But with the addition of epoxy resin, the decreasing trend of compressive strength of geopolymers was alleviated, and even the compressive strength of EGP30 increased (the compressive strength increased by 4.77MPa and 4.24MPa, respectively). The reason for this phenomenon was that the reaction between metakaolin and alkali excited solution was basically completed when EGP 0 curing for 1d, and the compressive strength had reached a high level; however the EGP 10, 20, and 30 groups did not complete the polycondensation reaction due to the presence of epoxy resin, and the excessive water also slowed down the polycondensation reaction; therefore the amount of geopolymer gels decreased, so did the compressive strength. However, the mechanical strength of EGP30 was significantly improved after soaking for 56 days, which may be due to the formation of the geopolymer gels; it made the structure dense and offset the microcrack expansion caused by seawater corrosion. After 28 days of curing, the compressive strength of all groups decreased because the geopolymer had completed the polycondensation, but as the curing days are gone, microcracks occurred and seawater corrosion also increased the expansion of cracks, but these cracks did not influence

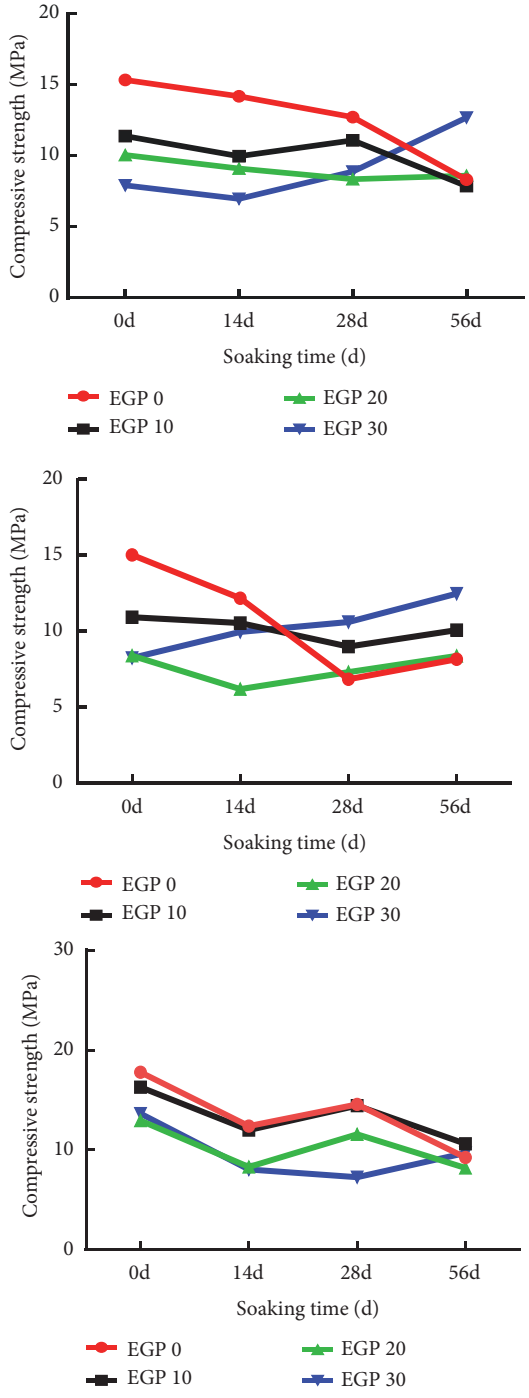

Figure 7: Compressive strength after curing for 1d, 3d, 28d and soaking for 56d.

the compressive strength in the early stage. Although the compressive strength of EGP 0-30 decreased by 8.55MPa, 5.66MPa, 4.76MPa, and 3.94MPa, respectively, with the addition of the epoxy resin, the seawater corrosion resistance of the geopolymer enhanced (see Table 5).

The X-ray diffraction pattern after seawater erosion for 56 days was shown in Figure 8. The metasilicate kaolin base polymer phase with epoxy resin was aluminosilicate, which

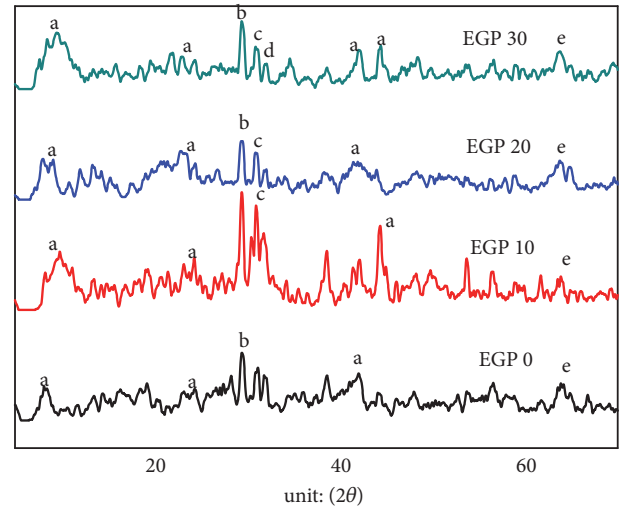

Figure 8: X-ray diffraction after seawater erosion for 56d.

Table 5: The phase corresponding to XRD Atlas.

Symbol	Mineral name	Chemical formula
a	Sodium aluminosilicate	$Na_3Al_3Si_5O_{14}$
b	Chabasite	$NaAlSi_3O_8$
c	Zeolite	$Na_6(AlSiO_4)_6$
d	Carnegieite	$NaAlSiO_4$
e	Cubicite	$Na(Si_2Al)O_6\ H_2O$

indicated that seawater erosion had no obvious influence on the material phase structure of the test piece. Metakaolin base polymer had good seawater corrosion resistance

4. Conclusion

The effect of epoxy resin on the compressive strength of geopolymers was investigated by experiments. The mechanism of the impact resistance of epoxy resin on geopolymers and the antiseawater performance of geopolymer with different epoxy resin concentrations were studied.

(1) The metakaolin base geopolymer mainly consists of an amorphous phase and a quartz phase. As the epoxy resin was added, the geopolymer did not form other phases.

(2) The epoxy resin could inhibit the polymerization reaction, and the compressive strength of the metakaolin-based geopolymer increased slowly. Compared with curing for 3d, the compressive strength growth rate of EGP 30 group after curing for 28 days was 65.34%.

(3) The antiseawater performance of epoxy resin metakaolin geopolymer was better, and the compressive strength enhanced by 4.77 MPa when curing for 1d and soaking for 56d.

Data Availability

The data used to support the findings of this study are included within the article. No additional unpublished data are available.

Conflicts of Interest

The authors declare that they have no conflicts of interest.

Acknowledgments

This work was supported by The Key State Laboratory of Coastal and Offshore Engineering (No. LP1720) and Liaoning Province Natural Science Foundation of China (No. 20170540143).

References

[1] H. W. Tian, W. H. Li, C. Z. Zong, and B. R. Hou, "Corrosion mechanism and research progress of anti-corrosion coatings for reinforced concrete used in marine environment," *Paint & Coatings Industry*, vol. 38, pp. 62–67, 2008 (Chinese).

[2] A. M. Aguirre and R. Mejía de Gutiérrez, "Durability of reinforced concrete exposed to aggressive conditions," *Materiales de Construcción*, vol. 63, no. 309, pp. 7–38, 2013.

[3] M. M. Al-Zahrani, S. U. Al-Dulaijan, M. Ibrahim, H. Saricimen, and F. M. Sharif, "Effect of waterproofing coatings on steel reinforcement corrosion and physical properties of concrete," *Cement and Concrete Composites*, vol. 24, no. 1, pp. 127–137, 2002.

[4] A. A. Almusallam, F. M. Khan, S. U. Dulaijan, and O. S. B. Al-Amoudi, "Effectiveness of surface coatings in improving concrete durability," *Cement and Concrete Composites*, vol. 25, no. 4-5, pp. 473–481, 2003.

[5] G. Batis and P. Pantazopoulou, "Advantages of the simultaneous use of corrosion inhibitors and inorganic coatings," in *Proceedings of the Second International Symposium on Cement and Concrete Technology*, vol. 24, pp. 6–10, 2000.

[6] C. Christodoulou, C. Goodier, S. Austin, J. Webb, and G. Glass, "Long-term performance of surface impregnation of reinforced concrete structures with silane," *Construction and Building Materials*, vol. 48, pp. 708–716, 2013.

[7] S. Sadati, M. Arezoumandi, and M. Shekarchi, "Long-term performance of concrete surface coatings in soil exposure of marine environments," *Construction and Building Materials*, vol. 94, pp. 656–663, 2015.

[8] J. Davidovits, "Geopolymers, man-made rock geosynthesis and the resulting development of very early high strength cement," *Journal of Materials Education*, vol. 16, pp. 91–139, 1994.

[9] J. Davidovits, *Geopolymer Chemistry and Applications*, Institute Geopolymer, Saint-Quentin, France, 3rd edition, 2011.

[10] G. Habert, J. B. D'Espinose De Lacaillerie, and N. Roussel, "An environmental evaluation of geopolymer based concrete production: Reviewing current research trends," *Journal of Cleaner Production*, vol. 19, no. 11, pp. 1229–1238, 2011.

[11] D. Hardjito, S. E. Wallah, D. M. J. Sumajouw, and B. V. Rangan, "On the development of fly ash-based geopolymer concrete," *ACI Materials Journal*, vol. 101, pp. 467–472, 2004.

[12] P. Duxson, J. L. Provis, G. C. Lukey, and J. S. J. van Deventer, "The role of inorganic polymer technology in the development of 'green concrete'," *Cement and Concrete Research*, vol. 37, no. 12, pp. 1590–1597, 2007.

[13] V. F. Barbosa and K. J. MacKenzie, "Synthesis and thermal behaviour of potassium sialate geopolymers," *Materials Letters*, vol. 57, no. 9-10, pp. 1477–1482, 2003.

[14] Z. Zhang, X. Yao, and H. Zhu, "Potential application of geopolymers as protection coatings for marine concreteI. Basic properties," *Applied Clay Science*, vol. 49, no. 1-2, pp. 1–6, 2010.

[15] A. Palomo, A. Macias, and Blanco., "Physical, Chemical and mechanical characterization of geopolymers," in *Proceedings of the 9th International Congress on the Chemistry of Cement*, vol. 5, pp. 505–511, 1992.

[16] P. Duxson, G. C. Lukey, and J. S. J. Van Deventer, "Physical evolution of Na-geopolymer derived from metakaolin up to 1000˚C," *Journal of Materials Science*, vol. 42, no. 9, pp. 3044–3054, 2007.

[17] A. Palomo, M. Blanco-Varela, M. Granizo, F. Puertas, T. Vazquez, and M. Grutzeck, "Chemical stability of cementitious materials based on metakaolin," *Cement and Concrete Research*, vol. 29, no. 7, pp. 997–1004, 1999.

[18] A. M. Aguirre-Guerrero, R. A. Robayo-Salazar, and R. M. de Gutiérrez, "A novel geopolymer application: Coatings to protect reinforced concrete against corrosion," *Applied Clay Science*, vol. 135, pp. 437–446, 2017.

[19] Z. Zhang, X. Yao, and H. Zhu, "Potential application of geopolymers as protection coatings for marine concreteII. Microstructure and anticorrosion mechanism," *Applied Clay Science*, vol. 49, no. 1-2, pp. 7–12, 2010.

[20] Y. S. Zhang, W. Sun, and Z. J. Li, "Preparation and microstructure of K-PSDS geopolymeric binder," *Colloids and Surfaces A: Physicochemical and Engineering Aspects*, vol. 302, no. 1-3, pp. 473–482, 2007.

[21] A. Nazari, A. Maghsoudpour, and J. G. Sanjayan, "Characteristics of boroaluminosilicate geopolymers," *Construction and Building Materials*, vol. 70, pp. 262–268, 2014.

[22] M. Criado, A. Palomo, and A. Fernández-Jiménez, "Alkali activation of fly ashes. Part 1: effect of curing conditions on the carbonation of the reaction products," *Fuel*, vol. 84, no. 16, pp. 2048–2054, 2005.

[23] C. E. White, K. Page, N. J. Henson, and J. L. Provis, "In situ synchrotron X-ray pair distribution function analysis of the early stages of gel formation in metakaolin-based geopolymers," *Applied Clay Science*, vol. 73, pp. 17–25, 2013.